

Measurements of ice deformation at the confluence area of Unteraargletscher, Bernese Alps, Switzerland

G. HILMAR GUDMUNDSSON,¹ ALMUT IKEN,² MARTIN FUNK¹

¹Versuchsanstalt für Wasserbau, Hydrologie und Glaziologie, ETH Zentrum, Gloriastrasse 37/39, CH-8092 Zürich, Switzerland

²Rockwinkelstrasse 35 A, D-28355 Bremen, Germany

ABSTRACT. An experimental study of ice deformation at the confluence area of Unteraargletscher, Bernese Alps, Switzerland, has been carried out. Surface velocities were measured by repeatedly surveying stakes and with the use of remote-sensing methods. The variation of the vertical strain rates with depth was measured in boreholes. The confluence center line is subjected to longitudinal horizontal extension, which is exceeded in magnitude by a concomitant transverse compression. Vertical strain rates change from positive (extension) at the surface to negative (compression) in the lowest layers of the glacier.

INTRODUCTION

The confluence of two glaciers is an ideal place to study the mechanics of ice deformation, as the glaciers must adjust themselves to a completely new bed geometry over a short distance of often only a few mean ice thicknesses. However, relatively few studies have been conducted on the ice mechanics of glacier confluences, the reason presumably being that the complexity of the flow field makes interpretations of field measurements difficult.

The most detailed experimental work done so far on the convergence of two glaciers seems to be that on Kaskawulsh Glacier, Yukon Territory, Canada, as part of the Icefield Ranges Research Project. Among other things, the bedrock topography, surface velocity, crevasses and morphological features were studied (Brecher, 1969; Clarke, 1969; Holdsworth, 1969a, b; Wagner, 1969a, b; Anderton, 1970; Dewart, 1970; Dozier, 1970; Ewing, 1970). The flow pattern of the confluence of Tyndall Glacier, southern Patagonia, has also been analyzed (Casassa, 1992; Kadota and others, 1992), and the formation and evolution of medial moraines has been investigated in papers by Anderton (1970), Eyles and Rogerson (1978), Gomez and Small (1985) and Vere and Benn (1989).

Theoretical work on the deformation and the stress field at the junction of two glaciers has been performed by Collins (1970). He used the techniques of slip-line theory and assumed a rigid/perfectly plastic material behavior of ice. Further assumptions included rigid "plug flow" movement of the ice above and below the confluence zone and plane strain deformation. Collins suggested that the dynamics of a confluence would introduce some surface modifications counteracted by the onset of "secondary flow", i.e. a small amount of circulating flow superimposed on the main flow. For a Y-shape junction this would be expressed in a downward flow component at the central part of the confluence area and in an upward-flow component close to the outer walls of the confluence area.

In this paper, the results of an experimental study of the confluence area of Unteraargletscher, Bernese Alps, Swit-

zerland, are described. The fieldwork consisted mainly of repeated surveyings of stakes and borehole measurements of the variation of the vertical velocity component with depth. Surface velocities of the confluence area of high (50 m) spatial resolution are presented and discussed. The properties of the flow are investigated with two-dimensional models in a separate paper (Gudmundsson, 1997c).

Setting

Finsteraar- and Lauteraargletscher are the two tributaries of Unteraargletscher (Fig. 1). They are both about 1 km wide and their surface velocities are similar in magnitude. Where they flow together they form an angle of roughly 100°. Unteraargletscher extends about 6 km eastwards from the confluence of Lauteraar- and Finsteraargletscher and has a mean width of 1 km and a mean slope of approximately 4°. The confluence itself, which lies within the ablation area, has an area of about 2 km² and is 2400 m a.s.l. All three glaciers are temperate.

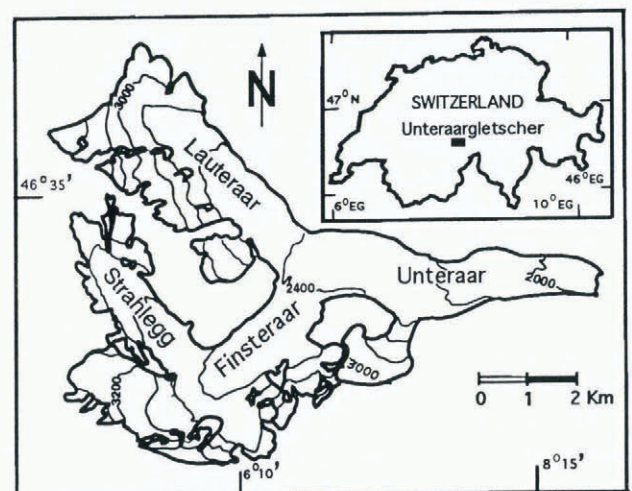


Fig. 1. Map of Strahlegg-, Lauteraar-, Finsteraar- and Unteraargletscher and their locations within Switzerland.

A conspicuous feature of Unteraargletscher is the large ice-cored medial moraine. It is overlain by a surficial rock detritus of typically 5–15 cm thickness. Within the area of the confluence, the medial moraine is 10–18 m high and 150 m wide. It becomes higher and wider in the down-flow direction, reaching a maximum height of about 25 m and a width of approximately 300 m. Further down-glacier the medial moraine gradually spreads out laterally and merges with the marginal morainic debris.

Within the confluence area, deep-reaching crevasses are found only close to its southeast edge. About 300 m from the junction point, the medial moraine is cut by a small number of wide crevasses lying perpendicular to the direction of flow.

Previous studies on Unteraargletscher

Unteraargletscher is one of the most comprehensively studied glaciers in the Alps. The beginning of quantitative glaciological measurements can be traced back to the work of Hugi in 1827 and Agassiz in 1841–46 (Hugi, 1830, 1842; Agassiz, 1847). Since 1924, systematic measurements of surface changes and velocities have been made each year (Flotron and Flotron, 1924–97). A comprehensive list of references to glaciological work relating to Unteraargletscher can be found in Zumbühl and Holzhauser (1988, 1990).

Flow behavior

The flow behavior of Unteraargletscher from 1845 to date is known in some detail (Haefeli, 1970). In 1845–46, velocities along two profiles were measured every month by Agassiz (1847) and his co-workers. One of the profiles was close to the confluence. Both profiles showed large seasonal velocity fluctuations, with their maximum velocities occurring in the period from mid-April until the end of June, and their minimum from the end of October until mid-January. The maximum velocities (averaged over a few days) were about 1.6 times larger than the mean annual velocities.

From 1969 until 1980, ice motion was studied by means of an automatic camera positioned about 2 km below the confluence (Flotron, 1973). Again, large seasonal velocity variations were found, with higher velocities during the summer. The summer velocities varied from year to year, but the winter velocities remained stable. In June 1975 the camera records were complemented by theodolite measurements at four transverse profiles. A number of uplift events interpreted as being due to increased water storage at the bed were observed (Iken and others, 1983). Recent measurements showed similar uplift events on Unteraargletscher, accompanied by strong lateral compression and vertical extension (Gudmundsson, 1996). A detailed analysis is necessary to determine whether the uplift is caused by strain events, water storage or both.

Bed topography

Parts of Finsteraar- and Lauteraargletscher and the whole of Unteraargletscher have been investigated by seismic reflection methods (Knecht and Süssstrunk, 1952) and radio-echo soundings (Funk and others, 1994). The bedrock geometry of Unteraargletscher is therefore known in detail.

RESULTS

During the second week of September 1991, four holes were

drilled with a hot-water jet at a location close to the medial moraine about 500 m down-glacier from the junction point (Fig. 2). The holes were only 10–20 m apart and had depths of 100–281 m. The total ice thickness at the drilling site is about 340 m. Air temperatures were above the freezing point, and considerable surface melting occurred during the day.

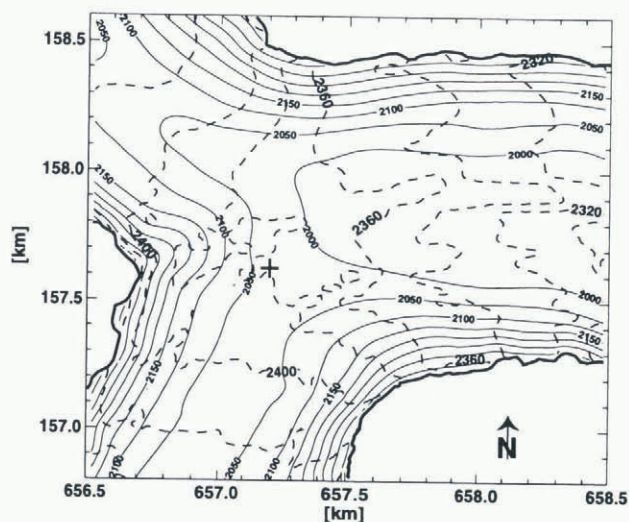


Fig. 2. Map of the confluence area, showing both surface (dashed lines) and bedrock (solid lines) topography. The solid cross shows the location of the 1991 drilling site.

Vertical strain rates

To gain information on vertical strain rates, three of the boreholes were equipped with magnetic rings, anchored on 1.5 m long aluminum tubes, at depths of 100, 150 and 200 m. The vertical movements of the magnetic rings were measured several times a day with respect to reference stakes at the surface. The absolute positions of the reference stakes were also measured with a theodolite situated on bedrock to the side of the glacier.

Vertical ice displacements were rather steady and surprisingly large: 1.39 ± 0.07 , 1.97 ± 0.27 and 2.19 ± 0.07 cm d⁻¹ for the rings at 100, 150 and 200 m depths, respectively (positive values indicate extension). The displacements of the rings at depths of 100 and 200 m are shown in Figure 3. Measurements of the ring at 150 m could not be continued as long as those of the other two rings. The installation and the measurements of the magnetic rings are described in more detail in Gudmundsson (1994b).

The mean vertical strain rate over the distance between the magnetic ring and the reference mark at the surface is a combination of vertical stretching and horizontal shear. On the basis of finite deformation theory, Harrison (1975) derived the formula

$$\dot{\epsilon} \approx \dot{\epsilon}_{zz} + 2\dot{\epsilon}_{xz} \sin \alpha + \dot{\epsilon}_{xz}^2 t,$$

for the strain rate $\dot{\epsilon}$ resulting both from the strain rate perpendicular to the surface and from shearing. The time interval between measurements was approximately 0.003 a, and $\sin \alpha \approx 0.05$. A reasonable value for the shear strain rates is $\dot{\epsilon}_{xz} \approx 0.05$ a⁻¹. (This estimate follows from an unpublished three-dimensional flow model of the confluence area; Gudmundsson, 1994b.) The contribution of shearing to borehole stretching is therefore less than 0.005 a⁻¹. Measured values

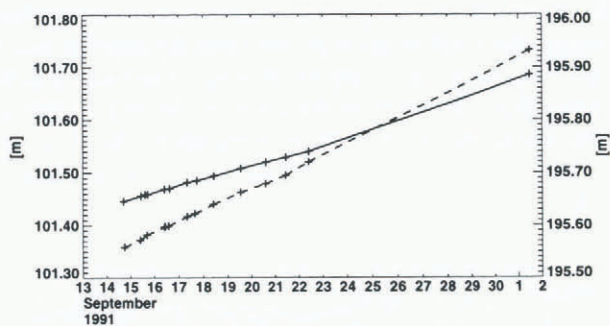


Fig. 3. Vertical displacements of magnetic rings at depths of 100 m (solid line) and 200 m (dashed line) with respect to the glacier surface, as functions of time. The symbols represent measured values. The errors associated with each measurement are estimated to be less than ± 1.5 mm, except for the last measurement on 1 October, for which the errors are of the order of ± 2 cm.

for $\dot{\epsilon}$ are considerably larger, so that $\dot{\epsilon} \approx \dot{\epsilon}_{zz}$. Hence, the contribution of shearing to the changes in distance between the surface reference mark and the magnetic ring can be ignored.

The movements of the reference marks at the surface relative to a fixed point outside the glacier were also measured, and they corresponded to an average thickening rate of 1.0 ± 0.5 cm d⁻¹. This relatively high error estimate as compared to the results obtained with the magnetic rings is caused by the fact that the measured vertical displacement is in part due to vertical stretching/compression and in part to the overall downward flow of the glacier. These two components can be separated only by estimating the average surface slope, which introduces some errors.

The measured vertical velocity profile is depicted in Figure 4. Measured values were interpolated by using a third-degree polynomial with weighting factors that are inversely proportional to the measurement errors. The most conspicuous feature is the maximum of v_z at approximately 220 m depth. The exact location of this maximum is some-

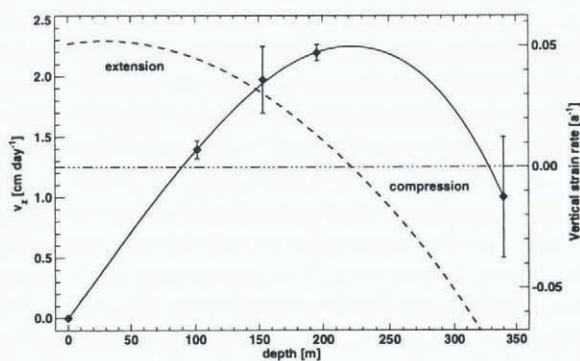


Fig. 4. Measured vertical ice velocity relative to the surface as a function of depth (solid line), and the corresponding variation of vertical strain rates $\dot{\epsilon}_{zz}$ with depth (dashed line). The solid curve is based on an interpolation of the measured velocities of magnetic rings in boreholes with respect to the surface (Fig. 3), and the total vertical movement of the surface with respect to a fixed reference point. Velocities are relative to the glacier surface, with positive values indicating downward movements. The vertical strain rate (dashed line) is the slope of the solid curve.

what uncertain as the curve is based on only five data points. However, it is beyond doubt that the vertical velocity increases with depth and then decreases again, causing a shift in strain rates from positive (extension) to negative (compression) somewhere between 195 and 340 m. Vertical strain rates obtained by differentiating the interpolation curve are also given in Figure 4. This essentially monotonic, but quadratic, variation of the vertical strain rates with depth should be contrasted with the assumption of a constant or linear variation of the strain rates with depth so often made in the glaciological literature (Paterson, 1994, p. 276–279).

Horizontal strain rates

The horizontal strain rate at the drilling site was determined by measuring the movements of five stakes set up as a square with one stake at the center. The distance from the center stake to the others was approximately 50 m. The stakes were surveyed four times during the winter of 1991–92, on 17 September and 10 October 1991, and 1 January and 4 April 1992. Strain rates for each interval were calculated by finding the best fit of the velocity of each stake to the expression

$$v_i = \beta_{0i} + \beta_{1i}x + \beta_{2i}y \quad \text{for } i = 1, 2$$

where v_i are the horizontal velocity components, x and y are the coordinates of the stake at which the velocity was measured, and the β_{ji} 's are regression coefficients.

From 17 September to 30 October 1991 the rate of deformation was considerably larger than during the two subsequent time periods. This seasonal strain-rate variation may have been caused by changes in geometry or a sudden change in boundary conditions related to changes in basal sliding distribution, the latter possibility being the preferred cause. The orientation of the principal compressive strain rates is approximately north–south (Fig. 5), and they exceed the concomitant east–west extension.

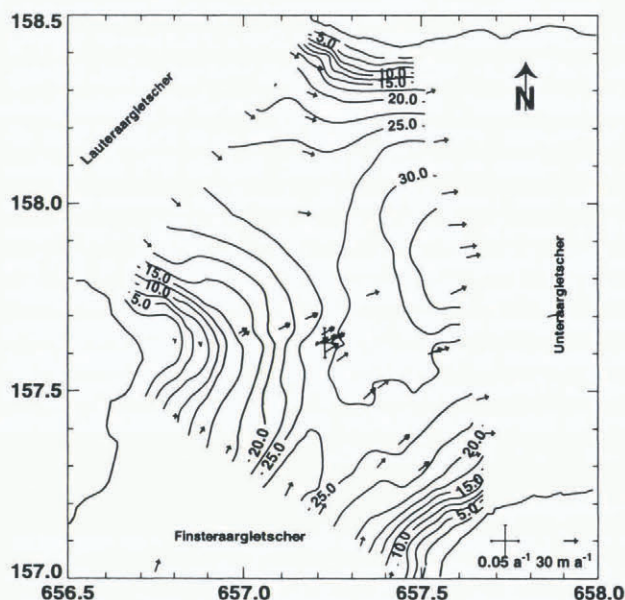


Fig. 5. Velocities and principal strain rates calculated from marker movements during the winters of 1991–92 and 1992–93. Vectors denote horizontal velocities; contour lines give the speed. The strain-rate cross is at the location of the drilling site. Contour interval is 2.5 m a^{-1} . Coordinates are in km.

Considerable surface melting took place during September 1991 and possibly the first week of October. On 30 October no melting occurred and the glacier was covered with fresh snow. This presumably led to a drop in water pressure and a consequent decrease in sliding velocity. Changes in sliding velocity will, for such a complicated geometry as that of a confluence area, almost inevitably lead to changes in the ice-deformation pattern.

No temporal strain-rate variations were observed during the winter, and the velocities of the markers did not change with time over this period. Hence, throughout the winter of 1991–92, sliding velocities did not change and were possibly even zero. No marginal sliding was observed during the winter, which suggests that if basal sliding takes place, it must be confined to the lower sections of the glacier bed. On the other hand there are indications of some marginal sliding taking place during the summer.

Surface velocities extracted from aerial photographs

Aerial photographs are taken of the Aaregletscher (the collective name for Finsteraar-, Lauteraar-, Unteraar- and Oberaargletscher) during late summer every year. By comparing two different stereo models generated at different times, the surface velocity field can be constructed (Flotron, 1979; Käab, 1996).

Figure 6 shows the surface velocity field of the confluence area, as extracted from a comparison of multitemporal stereo models from aerial photographs taken on 15 August 1989 and 20 August 1990. The velocity plot was generated by Bauder (1996) at VAW-ETHZ, Zürich, and digital terrain models from both years were made available by the engineering firm Flotron AG.

The vectors in Figure 6 represent the raw data. The contour lines of the horizontal speed were calculated from filtered velocities. The filtering of the velocities is explained below. Maximum annual velocities are about 45 m a^{-1} , the

maximum being reached close to the center of the confluence area where the ice thickness is greatest (Fig. 2). Surface velocities on Finsteraargletscher are somewhat larger than those of Lauteraargletscher, in general agreement with thickness differences. It is, however, questionable how much emphasis should be placed on the interpretation of annual velocities for a glacier which is known to exhibit large temporal variations in sliding velocity and hence in surface velocity. Since the boundary conditions change throughout the year (and the surface velocity with them) the average annual velocity field may never be realized for any particular period of time. The annual velocity distribution therefore reflects the sum of different physical processes realized at different times, but the sum itself may not correspond to any physical reality.

To obtain a better idea about annual surface velocity variations, an additional pair of aerial photographs, taken on 23 July 1991 by the Federal Cadastral Directorate, was used together with the aerial photographs from 22 August for surface velocity determination. The aerial photographs were evaluated by W. Schmid at VAW-ETHZ, and the resulting surface velocities can be seen in Figure 7. Note that although velocities of Unteraargletscher are known to vary on time-scales of days and weeks during spring and summer (Flotron, 1973; Iken and others, 1983; Gudmundsson, 1996), the averaged velocities over the time period 23 July–22 August 1991 will be referred to as summer velocities hereafter.

The maximum summer velocities of the confluence area are approximately 55 m a^{-1} . In the up-glacier direction towards Lauteraargletscher, the velocities decrease and increase again further upstream, whereas in the up-glacier direction towards Finsteraargletscher a continuing increase with distance is observed. On the west side of the confluence, close to the junction point, an extended area of large velocity gradients can be seen (Fig. 7). Along the north and south margins marginal sliding seems to take place.

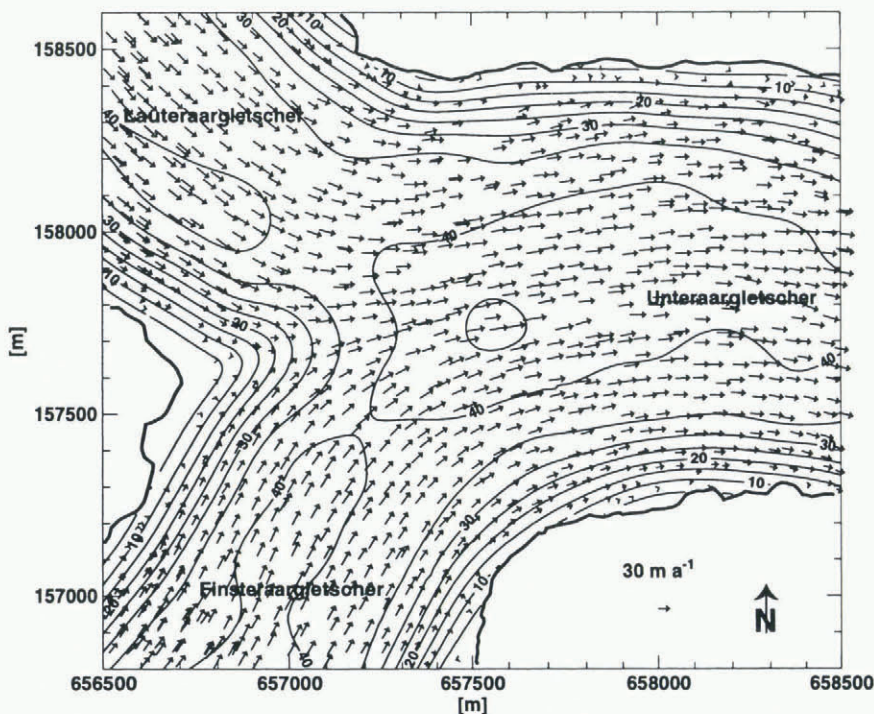


Fig. 6. Annual horizontal surface velocities derived from aerial photographs taken on 22 August 1990 and 20 August 1991. The contour interval is 5 m a^{-1} . Coordinates are in meters.

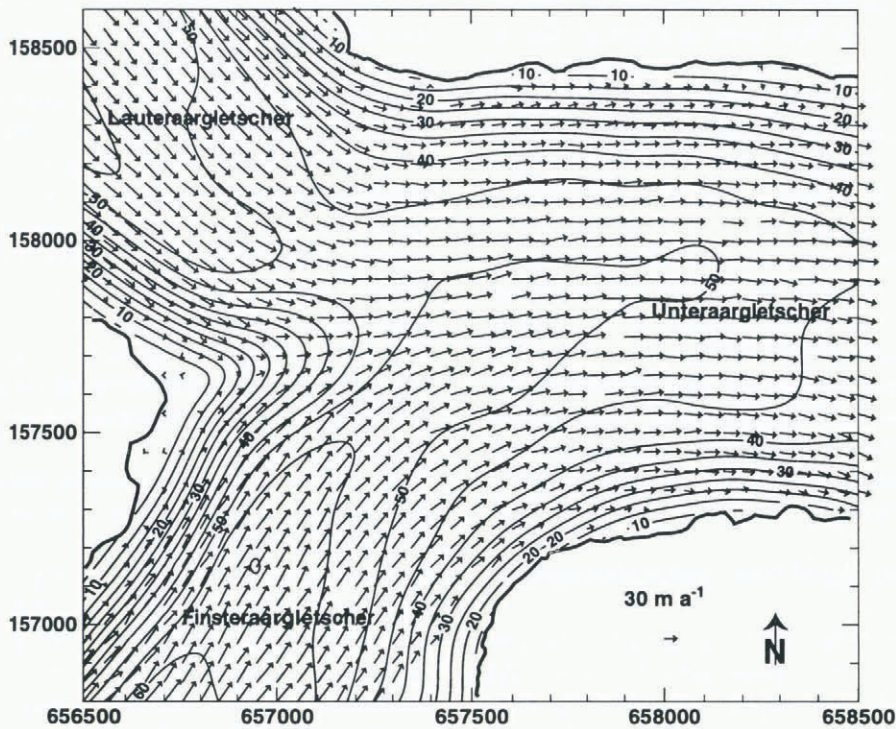


Fig. 7. Horizontal summer surface velocities extracted from aerial photographs for the period 23 July–22 August 1991. The contour interval is 5 m a^{-1} . Coordinates are in meters.

In situ velocity measurements

During winter the snow cover renders the surface more or less featureless, and ice velocities cannot be extracted from aerial photogrammetry. Winter velocities were therefore calculated from repeated surveying of stakes. Altogether, 78 stakes were drilled into the ice, of which 25 were installed in autumn 1991. These were repetitively surveyed on 30 October 1991, 16 January 1992 and 17–19 April 1992. Additional markers were installed during the radio-echo sounding survey of April 1992 and measured for about 3 d. Markers were reinstalled in autumn 1992 and measured on 1 December 1992 and 19 January 1993. The results of all these measurements are tabulated in Gudmundsson (1994).

Surface velocities did not change during the period October 1991–April 1992. Velocities during the winter of 1992–93 were, within observational errors, the same as those of winter 1991–92. Figure 5 depicts marker velocities during the winters of 1991–92 and 1992–93. Several additional markers, outside the confluence area, are not shown. Interpolation of the rather limited number of velocity measurements was done with the Akima interpolation algorithm (Akima, 1978).

There is no indication of marginal sliding during the winter months. This observation was used in the interpolation of the surface speed (Fig. 5) by setting the velocities along the boundary to zero. Extrapolation of marker velocities toward the glacier boundary may depend to some extent on this assumption. The velocities within the confluence area are, on the other hand, not affected by this assumption.

Because of largely reduced or even totally absent basal sliding, winter velocities are approximately 75% of summer values. However, a qualitative difference also can be seen by comparing Figures 5 and 7. A clear velocity maximum appears in the winter velocities close to the confluence center,

but not in the summer velocities. This is a good example of seasonal variation of the deformation profile across and along a glacier surface and shows, together with the temporal change in surface strain rates, how temporal basal sliding variations can affect the internal deformation pattern of the ice. Temporal changes in deformation rates may be especially marked for a confluence, because a relatively large contact area between the ice and the bedrock over which basal sliding can occur transforms at the junction point into an ice–ice contact area. Along the ice–ice contact area, no or negligible relative slip motion takes place. It is also clear that the three-dimensional geometry of the confluence makes a simple plug-flow velocity field impossible.

Surface strain-rate pattern extracted from aerial photography

Optimal filtering of measured surface velocities

Possibly the most straightforward method of estimating horizontal strain rates ($\dot{\epsilon}_{ij}$) from measured surface velocities (v_i) would be to interpolate the velocities to the nodes of a square grid, and then to approximate the expression $\dot{\epsilon}_{ij} = \frac{1}{2}(v_{i,j} + v_{j,i})$ through finite differences. This method will not work without some adjustment, however, if random data errors introduce apparent spatial velocity variations of comparable magnitude to the actual (noise-free) velocity variations of the glacier.

Because the spatial distance between measurements was about 50 m, and the velocity error is estimated to be about 0.3 m a^{-1} , the error in the strain-rate estimate over this distance will be approximately $\sqrt{2} \times 0.3/50 = 0.008 \text{ a}^{-1}$, which is comparable in magnitude to the expected surface-strain rates. Strain rates calculated over larger distances can be estimated more accurately, but these long-wavelength strain-rate variations will not be detectable in the noise associated with the short-wavelength strain-rate variations unless some filtering is done. If vertical strain rates along the surface are

to be calculated with the help of the incompressibility condition, an effective and reliable method of error reduction is especially important, as the two horizontal strain-rate components tend to be of similar but opposite magnitude.

Because the errors depend strongly on the wavelength of the spatial strain-rate variation — decreasing inversely with distance — a wavelength-dependent filter can be used to effectively eliminate the high-frequency errors. To this end the two-dimensional Fourier transforms of the velocity distributions $v_x(x, y)$ and $v_y(x, y)$ were calculated, and an optimal Wiener filter,

$$W(k) = \frac{|S(k)|^2}{|S(k)|^2 + |N(k)|^2},$$

constructed, where $k = \sqrt{k_x^2 + k_y^2}$, and k_x and k_y are the horizontal wavenumbers. $N(k)$ and $S(k)$ are the error and the noise models determined from the power spectrum of the measured velocities (Rabiner and Gold, 1975; Press and others, 1996). The filter $W(k)$ was applied to the Fourier-transformed velocities. The strain rates $\dot{\epsilon}_{ij}(k_x, k_y)$ were calculated directly in frequency space by forming the corresponding products of the transformed velocities with the wavenumbers. Calculation of horizontal strain rates is faster with this method than with either locally adaptive linear-regression models (Bauder, 1996) or the method of Nye (1952) (which has often been used in the glaciological literature), and the results are less prone to errors in the data. It should be stressed that filtering of the velocity data was absolutely imperative for extracting information on the strain-rate variation across the glacier surface from the surface velocities.

Characteristics of surface strain-rate patterns

The surface strain rates of the confluence area for the time periods 23 July–22 August 1991 and 22 August 1990–20

August 1991 are shown in Figures 8 and 9, respectively. These surface strain rates were calculated along a 50 m square grid from the velocities shown in Figures 6 and 7. Vertical strain rates were calculated from the incompressibility condition at all gridpoints where at least eight velocity measurements were available within a radius of 95 m.

Although some differences are detectable, the main features of Figures 8 and 9 are the same. Friction along the margins gives rise to zones of high horizontal shear but negligible vertical strain rates. Close to the junction point, where Lauteraar- and Finsteraargletscher converge, the center line is subjected to transverse compression and longitudinal extension. This is especially prominent over a roughly circular area, situated about 500 m down-flow of the junction point, where the transverse compression greatly exceeds the longitudinal extension in magnitude, resulting in a considerable vertical extension at the surface. In Figure 9, two points with local maxima in vertical surface strain rates can be identified, whereas in Figure 8, due to the lack of data, only one such point can be discovered. In agreement with the results from borehole measurements mentioned above, the transverse compression outweighs the longitudinal extension, causing a considerable vertical stretching along the surface.

In the down-flow direction, the strain-rate regime along the center line changes progressively towards a predominantly longitudinal compression, which is the expected state of flow for an ablation area (Nye, 1952). As a result, vertical strain rates are mostly positive, with two notable exceptions, both of which result from surface topographic undulations.

On Unteraargletscher a narrow east–west-extending zone of vertical compression can be seen in Figure 9. This zone coincides with the medial moraine, and this vertical compression and transverse extension is presumably an ex-

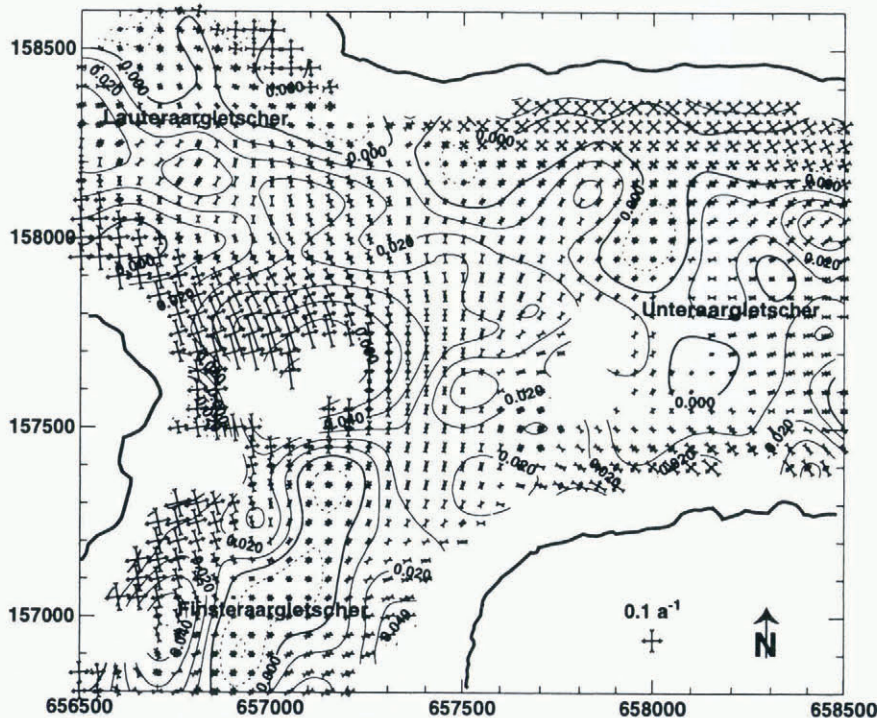


Fig. 8. Horizontal surface strain rates of the confluence area of Unteraargletscher, calculated from filtered velocities for the time period 23 July–22 August 1991 (Fig. 7). Contour lines represent vertical strain rates calculated by using the incompressibility condition, $\dot{\epsilon}_{ii} = 0$. Negative contours are drawn with dotted lines, and positive ones with solid lines. The contour interval is 0.01 a^{-1} . Coordinates are in meters.

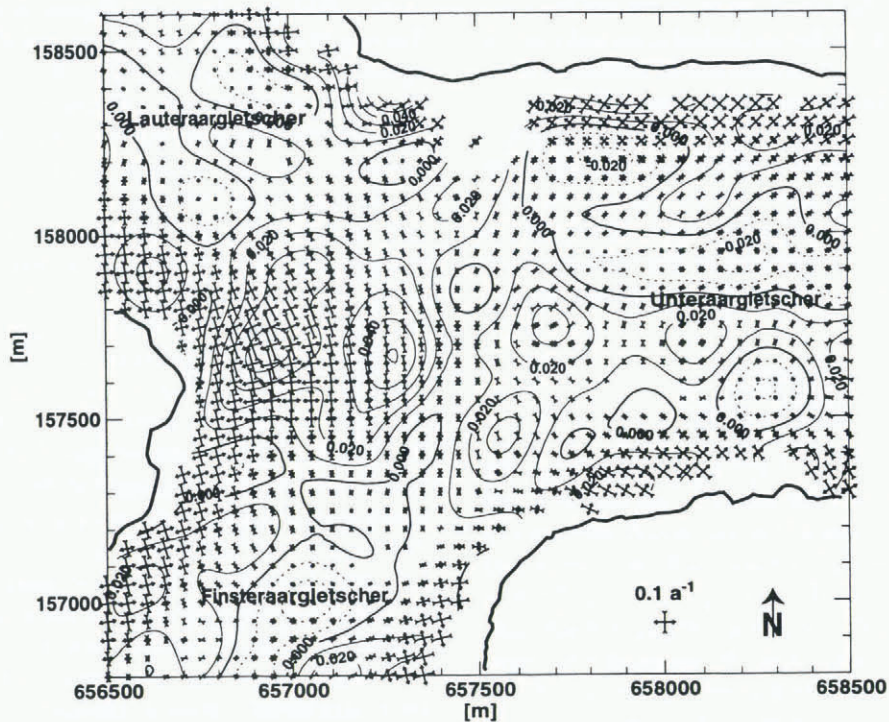


Fig. 9. Surface strain rates, derived from filtered surface velocities for the time period 22 August 1990–20 August 1991 (Fig. 6). Contour lines represent vertical strain rates. The contour interval is 0.01 a^{-1} . Coordinates are in meters.

pression of the lateral disintegration of the moraine itself. This transverse diffusion of surface features cannot be observed close to the junction point, because it is masked by the strong ice deformation caused by the flow dynamics of the confluence. Not only the ice velocities but also the internal ice-deformational pattern changes over the course of a year (cf. Figs 8 and 9). It is important to realize that it is the differential ablation, caused by the supraglacial debris cover, which is responsible for the build-up of the medial moraine, and not the convergent flow of the confluence area, as can be seen from the fact that (1) the medial moraine is limited to the debris-covered glacier surface, and (2) the zone of transverse compression has a much larger transverse extent than the medial moraine.

Directly south of the narrow east–west-extending zone of vertical compression, a parallel running zone of vertical extension and transverse compression can be identified (Fig. 9), which coincides with a surface depression. This zone is the only debris-free section of Unteraargletscher south of the medial moraine, and the surface depression results from a combination of differential ablation and the erosive effects of supraglacial streams, which form there every spring and exist throughout the summer. This zone is therefore in some respects an “inverse” medial moraine, with the corresponding inverted deformational pattern with respect to the medial moraine. Although it is an interesting fact that diffusion of these small surface undulations, having transverse dimensions of only about 150 m, can be retrieved and demonstrated with the help of aerial photographs, an accurate estimate of the rate of deformation will presumably only be possible through direct field measurements.

Some of the features seen in Figures 8 and 9, such as the small zones of vertical compression found along the center lines of Lauteraar- and Finsteraargletscher, where horizontal strain rates are almost zero, may not be real and are most likely caused by measurement errors. Care must also be

taken in interpreting some of the strain-rate patterns of the marginal zones where only a limited number of data points were available.

SUMMARY AND CONCLUSIONS

The main features of the surface strain-rate regime are easy to explain. Along the center line (which is considered to coincide with the medial moraine), the velocity increases as the ice moves from the junction point toward the center of the confluence. The medial moraine is, therefore, subjected to longitudinal extension. The transverse compression follows from the longitudinal extension, and the change in mean flow direction of the two converging arms within the confluence area. Practically identical results with respect to surface strain-rate pattern were found on Kaskawulsh Glacier, which shows that this kind of strain-rate regime is not exclusive to the confluence of Unteraargletscher.

Vertical strain rates integrated over depth must be positive below the medial moraine as long as ice thickness increases in the flow direction. This will in general be the case for the distance from the junction point to the confluence center. Because surface longitudinal and average vertical strain rates must be positive, it follows from the incompressibility assumption that the surface-transverse compression will in general be larger than the surface-longitudinal extension.

Summarizing, it is suggested that the overall strain-rate regime in a confluence can be understood in terms of three different mechanisms: (1) the effective ice-thickening in the flow direction along the medial moraine from the junction point toward the center; (2) the change in the mean flow direction of the two converging arms as the confluence area is approached; and (3) a velocity increase along the medial moraine from the junction point toward the confluence center.

The vertical strain-rate variation with depth is surprisingly complicated. The observed reversal from extensive to compressive flow with increasing depth is, at first sight, somewhat surprising and requires an explanation. Although the characteristics of basal flow can be quite complicated (Gudmundsson, 1997a, b), it must be expected, in general terms, that going from the glacier surface towards the glacier bed, the dip of the velocity vector will change slowly towards the dip of the bed–rock interface. If the dip of the velocity vector along the surface is less than that along the basal ice–rock interface, the result will be a vertical flow divergence and a vertical extension. The vertical component of the velocity vector will, hence, at first increase with depth. If no or negligible basal sliding takes place, the basal velocity, and in particular the vertical component of the basal velocity, must be zero. It follows that the down-flow velocity component must eventually start to decrease from a finite value toward zero as the bed is approached, leading to a vertical compression. This could explain the observed vertical compression, but the problem with this explanation is the fact that during the time period over which measurements of the vertical strain-rate variation were taken, considerable sliding took place. It is not clear what effect basal sliding will in general have on the vertical velocity profile. For the special case of sliding without friction, it can be shown (Gudmundsson, 1997c) that the vertical velocity component increases all the way down to the bed–rock interface, and that as a result, no zone of vertical compression develops. Hence, it is clear that the vertical strain-rate variation must be expected to depend on the exact form of the basal sliding law, and it must be concluded that, with respect to the observed vertical strain-rate variation, a no-slip boundary condition is more appropriate than a free-slip boundary condition.

Abrasion depends, among other things, on the rate of flow towards the bed (Gilbert, 1906; Hallet, 1981). The vertical convergence of the basal ice of the confluence area renders erosion of the glacier bed through abrasion possible. This could, in principle, lead to enhanced erosion with respect to the surrounding areas, but there is no indication of this occurring over the confluence of Lauteraar- and Finsteraargletscher, and the glacier bed shows no indications of overdeepened areas (Funk and others, 1994).

ACKNOWLEDGEMENTS

Research funding was provided by the Swiss National Science Foundation, grant No. 20-29619.90. A number of people assisted in gathering the data presented here. Special thanks are given to A. Abe-Ouchi, H. Bösch, K. Fabri, M. Lüthi, B. Nedela and the late W. Schmid. Careful reviews by K. Hutter, U. Fischer and two anonymous reviewers stimulated many improvements in the presentation of the paper.

REFERENCES

- Agassiz, L. 1847. *Système glaciaire ou recherches sur les glaciers, leur mécanisme, leur ancienne extension et le rôle qu'ils ont joué dans l'histoire de la terre. Première partie. Nouvelles études et expériences sur les glaciers actuels, leur structure, leur progression et leur action physique sur le sol.* Paris, Victor Masson.
- Akima, H. 1978. A method of bivariate interpolation and smooth surface fitting for irregularly distributed data points. *ACM Trans. Math. Software*, **4**, 148–159.
- Anderton, P.W. 1970. Deformation of surface ice at a glacier confluence, Kaskawulsh Glacier. In Bushnell, V.C. and R.H. Ragle, eds. *Icefield Ranges Research Project; Scientific Results. Vol. 2.* Montréal, Que., Arctic Institute of North America; New York, American Geographical Society, 59–76.
- Bauder, A. 1996. Massenbilanzmodellierungen mit photogrammetrischen Messungen und eismechanischen Berechnungen am Beispiel des Unteraargletschers. (Diplomarbeit, Eidgenössische Technische Hochschule, Zürich, Versuchsanstalt für Wasserbau, Hydrologie und Glaziologie.)
- Brecher, H.H. 1969. Surface velocity measurements on the Kaskawulsh Glacier. In Bushnell, V.C. and R.H. Ragle, eds. *Icefield Ranges Research Project; Scientific Results. Vol. 1.* Montréal, Que., Arctic Institute of North America; New York, American Geographical Society, 127–143.
- Casassa, G. 1992. Foliation on Tyndall Glacier, southern Patagonia. *Bull. Glacier Res.* **10**, 75–77.
- Clarke, G.K.C. 1969. Geophysical measurements on the Kaskawulsh and Hubbard Glaciers. In Bushnell, V.C. and R.H. Ragle, eds. *Icefield Ranges Research Project; Scientific Results. Vol. 1.* Montréal, Que., Arctic Institute of North America; New York, American Geographical Society, 89–106.
- Collins, I.F. 1970. A slip-line field analysis of the deformation at the confluence of two glacier streams. *J. Glaciol.*, **9**(56), 169–193.
- Dewart, G. 1970. Seismic investigation of ice properties and bedrock topography at the confluence of the north and central arms of the Kaskawulsh Glacier. In Bushnell, V.C. and R.H. Ragle, eds. *Icefield Ranges Research Project; Scientific Results. Vol. 2.* Montréal, Que., Arctic Institute of North America; New York, American Geographical Society, 77–102.
- Dozier, J. 1970. Channel adjustments in supraglacial streams. In Loomis, S.R., J. Dozier and K.L. Ewing, eds. *Studies of morphology and stream action on ablating ice.* Montréal, Que., Arctic Institute of North America, 67–117. (AINA Research Paper 57.)
- Ewing, K. 1970. Supraglacial streams on the Kaskawulsh Glacier, Yukon Territory. In Loomis, S.R., J. Dozier and K.J. Ewing, eds. *Studies of morphology and stream action on ablating ice.* Montréal, Que., Arctic Institute of North America, 119–167. (AINA Research Paper 57.)
- Eyles, N. and R.J. Rogerson. 1978. A framework for the investigation of medial moraine formation: Austerdalsbreen, Norway, and Berendon Glacier, British Columbia, Canada. *J. Glaciol.*, **20**(82), 99–113.
- Flotron, A. 1973. Photogrammetrische Messung von Gletscherbewegungen mit automatischer Kamera. *Vermessung, Photogrammetrie, Kulturtechnik*, **1973**(1), 15–17.
- Flotron, A. 1979. Verschiebungsmessungen aus Luftbildern. *Eidg. Tech. Hochschule, Zürich, Versuchsanst. Wasserbau, Hydrol. Glaziol. Mitt.*, **41**, 39–44.
- Flotron, A., Sr and A. Flotron, Jr. 1924–97. *Jährliche Berichte über die Ergebnisse der Gletschermessungen im Auftrag der Kraftwerke Oberhasli.* Kraftwerke Oberhasli.
- Funk, M., G.H. Gudmundsson and F. Hermann. 1995. Geometry of the glacier bed of the Unteraargletscher, Bernese Alps, Switzerland. *Zeitschrift für Glaziologie und Glazialgeologie*, **30**, 187–194.
- Gilbert, G.K. 1906. Crescentic gouges on glaciated surfaces. *Geol. Soc. Am. Bull.*, **17**, 303–316.
- Gomez, B. and R.J. Small. 1985. Medial moraines of the Haut Glacier d'Arolla, Valais, Switzerland: debris supply and implications for moraine formation. *J. Glaciol.*, **31**(109), 303–307.
- Gudmundsson, G.H. 1994. Converging glacier flow—a case study: the Unteraargletscher. *Eidg. Tech. Hochschule, Zürich, Versuchsanst. Wasserbau, Hydrol. Glaziol. Mitt.* 131.
- Gudmundsson, G.H. 1996. New observations of uplift events on Unteraargletscher. [Abstract.] *EOS*, **77**(46), Fall Meeting Supplement, F213.
- Gudmundsson, G.H. 1997a. Basal flow characteristics of a linear medium sliding frictionless over small bedrock undulations. *J. Glaciol.*, **43**(143), 71–79.
- Gudmundsson, G.H. 1997b. Basal flow characteristics of a non-linear flow sliding frictionless over strongly undulating bedrock. *J. Glaciol.*, **43**(143), 80–89.
- Gudmundsson, G.H. 1997c. Ice deformation at the confluence area of two glaciers investigated with conceptual map-plane and flowline models. *J. Glaciol.*, **43**(145), 537–547.
- Haefeli, R. 1970. Changes in the behaviour of the Unteraargletscher in the last 125 years. *J. Glaciol.*, **9**(56), 195–212.
- Hallet, B. 1981. Glacial abrasion and sliding: their dependence on the debris concentration in basal ice. *Ann. Glaciol.*, **2**, 23–28.
- Harrison, W.D. 1975. A measurement of surface-perpendicular strain-rate in a glacier. *J. Glaciol.*, **14**(70), 31–37.
- Holdsworth, G. 1969a. An examination and analysis of the formation of transverse crevasses, Kaskawulsh Glacier. In Bushnell, V.C. and R.H. Ragle, eds. *Icefield Ranges Research Project; Scientific Results. Vol. 1.* Montréal, Que., Arctic Institute of North America; New York, American Geographical Society, 109–125.
- Holdsworth, G. 1969b. Primary transverse crevasses. *J. Glaciol.*, **8**(52), 107–129.
- Hugi, F.J. 1830. *Naturhistorische Alpenreise.* Solothurn, Amiet-Lutiger.

- Hugi, F.J. 1842. *Über das Wesen der Gletscher*. Stuttgart and Tübingen, J.G. Cotta'scher Verlag.
- Iken, A., H. Röthlisberger, A. Flotron and W. Haeblerli. 1983. The uplift of Unteraargletscher at the beginning of the melt season — a consequence of water storage at the bed? *J. Glaciol.*, **29**(101), 28–47.
- Kääb, A. 1996. Photogrammetrische Analyse zur Früherkennung gletscher- und permafrostbedingter Naturgefahren im Hochgebirge. *Eidg. Tech. Hochschule, Zürich. Versuchsinst. Wasserbau, Hydrol. Glaziol. Mitt.* 145.
- Kadota, T., R. Naruse, P. Skvarca and M. Aniya. 1992. Ice flow and surface lowering of Tyndall Glacier, southern Patagonia. *Bull. Glacier Res.* 10, 63–68.
- Knecht, H. and A. Süssstrunk. 1952. *Bericht über die seismischen Sondierung des schweizerischen Gletscherkommission auf dem Unteraargletscher, 1936–1950*. Sion, Switzerland, Grande Dixence S.A. (Bericht 512.)
- Nye, J. F. 1952. The mechanics of glacier flow. *J. Glaciol.*, **2**(12), 82–93.
- Paterson, W. S. B. 1994. *The physics of glaciers. Third edition*. Oxford, etc., Elsevier.
- Press, W. H., S. A. Teukolsky, W. T. Vetterling and B. P. Flannery. 1996. *Numerical recipes in FORTRAN 77: the art of scientific computing. Second edition*. Cambridge, Cambridge University Press.
- Rabiner, L. R. and B. Gold. 1975. *Theory and application of digital signal processing*. Englewood Cliffs, NJ, Prentice-Hall.
- Vere, D. M. and D. I. Benn. 1989. Structure and debris characteristics of medial moraines in Jotunheimen, Norway: implications for moraine classification. *J. Glaciol.*, **35**(120), 276–280.
- Wagner, W. P. 1969a. Description and evolution of snow and ice features and snow surface forms on the Kaskawulsh Glacier. In Bushnell, V. C. and R. H. Ragle, eds. *Icefield Ranges Research Project; Scientific Results. Vol. 1*. Montréal, Que., Arctic Institute of North America; New York, American Geographical Society, 51–53.
- Wagner, W. P. 1969b. Snow facies and stratigraphy on the Kaskawulsh Glacier. In Bushnell, V. C. and R. H. Ragle, eds. *Icefield Ranges Research Project; Scientific Results. Vol. 1*. Montréal, Que., Arctic Institute of North America; New York, American Geographical Society, 55–62.
- Zumbühl, H. J. and H. Holzhauser. 1988. Alpengletscher in der Kleinen Eiszeit. *Die Alpen*, **64**(3), 129–322.
- Zumbühl, H. J. and H. Holzhauser. 1990. Alpengletscher in der Kleinen Eiszeit — Katalog und ¹⁴C-Dokumentation. *Geogr. Bernesia*, **31** (Supplement to *Die Alpen*, **64**(3), 1988).

MS received 18 April 1997 and accepted in revised form 16 June 1997